JOURNAL OF APPLIED ELECTROCHEMISTRY 23 (1993) 1132–1138

Corrosion and hydrogen surface embrittlement inhibition of amorphous FeBSiC alloy in molar HCl by diortho-aminodiphenyldisulphane (DOAPD)

S. KERTIT, J. ARIDE

Laboratoire de Physico-chimie des Matériaux, Ecole Normale Supérieure, B.P. 5118, Takaddoum, Rabat, Morocco

A. BEN-BACHIR, A. SRHIRI

Laboratoire d'Electrochimie, Faculté des Sciences, Université Ibn-Tofail, Kénitra, Morocco

M. ETMAN

Laboratoire d'Electrochimie des Interfaces du CNRS, 1 Place Aristide Briand, 92195 Meudon Cédex, France

Received 18 August 1992; revised 9 February 1993

The mode of corrosion inhibition of amorphous alloys due to diorthoaminodiphenyldisulphane (DOAPD) in molar HCl is studied through solution analysis and electrochemical steady state and transient measurements. DOAPD acts on the cathodic reaction without changing the mechanism of the hydrogen reduction reaction on the surface of the amorphous alloy electrode. The efficiency of corrosion inhibition depends on both the concentration of DOAPD and the potential of the electrode. The addition of 10^{-4} M DOAPD to 1 M HCl increases the impedance and decreases the capacity of the double layer. From the comparison of results with those obtained using other organic compounds, it is shown that DOAPD is the best inhibitor. A correlation between the efficiency of corrosion inhibition of DOAPD and its molecular structure is established. A schematic representation of the surface coverage due to different action modes of DOAPD cations is presented. Evidence is revealed for a double rôle of DOAPD in the decrease of corrosion and in hydrogen penetration. The schematic representation proposed explains why the mechanism of hydrogen reduction reaction is the same in the absence and in the presence of DOAPD.

1. Introduction

Amorphous alloys which show significant corrosion resistance are those based on Fe, Co, Ni and containing Cr and metalloids such as P, C, B or Si [1–4]. Amorphous alloys without Cr have little resistance to corrosion and to hydrogen embrittlement [5, 6]. The electrochemical behaviour of amorphous alloy electrodes depends on their structure and chemical composition [7, 8]. A study of the effect of organic compounds on the corrosion inhibition and on the embrittlement of the alloys due to hydrogen penetration seemed necessary.

The low resistance to corrosion and to hydrogen penetration into the alloys FeBSi and FeBSiC in 1 M HCl has been reported [9, 10]. Kertit *et al.* were the first to study the effect of added organic compounds on the corrosion and hydrogen penetration into the amorphous electrodes FeBSi and FeBSiC in 1 M HCl [11]. The efficiency of corrosion inhibition of diorthoaminodiphenyldisulphane (DOAPD) was determined from the current–voltage characteristics, loss of weight and from observations of the surface state of the electrode. Initial results have been published [9, 10] and the most important conclusions are as follows:

(i) Corrosion inhibition efficiency of DOAPD increases with concentration and attains a maximum at a critical value of 10^{-4} M. Inhibitor concentrations higher than 10^{-4} M lead to a decrease in corrosion inhibition efficiency accompanied by an increase in the cathodic current with respect to the current observed with the blank.

(ii) DOAPD is absorbed according to a Langmuir adsorption model.

(iii) Addition of DOAPD decreases hydrogen penetration into the amorphous alloy.

(iv) Inhibition efficiency of DOAPD is temperature-independent.

The aim of the present work is to clarify the mechanism of the processes occurring on the electrode in the absence and in the presence of DOAPD in 1 M HCl, to establish a correlation between the inhibition efficiency of DOAPD and its molecular structure and to propose a model for DOAPD

0021-891X

adsorption on the surface of FeBSiC amorphous electrodes in 1 M HCl.

The action of corrosion inhibition due to DOAPD is compared to the action of other organic compounds of the same family such as aniline, phenol, benzene and orthoaminothiophenol (OATP).

The electrochemical behaviour of the interface FeBSiC/1 M HCl in the absence and in the presence of DOAPD has been studied through the current–potential relationships, gravimetric analysis and electrochemical impedance measurements.

2. Experimental details

The experimental conditions have been described previously [9]. The FeBiSiC amorphous alloy, in the form of a tape, was prepared by a high speed quenching technique (melt-spinning) [10]. The side in contact with the cylinder onto which the tape was rolled during the preparation was matt while the reverse side was bright. For the electrochemical measurements, a three-electrode electrolysis cell was used. The temperature was thermostatically controlled at $24 \pm 1°C$. The working electrode, in the form of a disc, was cut from the amorphous tape and pressed onto a hollow steel support filled with a chemically inert resin. Electrode potentials were measured with respect to a saturated calomel electrode (SCE). The counter electrode was platinum with a surface area much higher than the working electrode. Prior to electrochemical measurements, the working electrode was cleaned with acetone and then washed with distilled water and dried in air. Before recording the cathodic current-potential characteristics, the working electrode was first activated at −800 mV vs SCE for 15 min. However, anodic polarization curves were recorded after the electrode was maintained at E_{corr} for a period of 30 min prior to measurements.

The electrochemical impedance measurements were performed using a transfer function analyser, (Schlumberger Solartron 1250) and a potentiostat (Solartron 1286). The galvanostatic electrochemical impedance measurements covered a frequency domain between 63.09 kHz and 10 mHz with five points per decade.

In the present work gravimetric measurements were carried out in a double walled Pyrex glass cell at $24 \pm 1°C$. The corrosion rate was determined by measuring the quantity of iron passed into the solution by atomic absorption spectrometry.

The electrolyte was 1 M HCl prepared from analytical grade reagents and bidistilled water. It was de-aerated by bubbling purified nitrogen for 1 h. The solution was magnetically stirred. The studied organic compounds were 'Merck' products. Preparation and identification of DOAPD are described elsewhere [10].

3. Results

In addition to DOAPD, the other organic compounds studied were benzene, phenol, aniline and orthoaminothiophenol (OATP). Their corrosion inhibition efficiency, $E(\%)$, is defined by

$$E(\%) = \frac{(i' - i)}{i'} \times 100 \qquad (1)$$

where i' and i represent, respectively, the corrosion current density in the absence and in the presence of the organic compound in 1 M HCl. The corrosion current densities were determined by extrapolation of Tafel lines.

The corrosion inhibition efficiency of DOAPD was compared to that of the other compounds. Positive value of $E(\%)$ indicate corrosion inhibition while negative values indicate increased corrosion (Table 1).

The current-potential characteristics of the cathodic and anodic polarization of the amorphous alloy/HCl interface in the absence and in the presence of the organic compounds (10^{-4} M) are represented in Fig. 1. Values of electrochemical parameters resulting from these Figures are given in Table 1.

Current-potential characteristics resulting from cathodic polarization gave rise to Tafel lines (Fig. 1(a)) indicating that the hydrogen evolution reaction is activation controlled. The addition of the organic compounds to the corrosive medium does not change the cathodic Tafel slope; this implies that the hydrogen reduction reaction on the surface of the FeBSiC electrode is not modified by the addition of organic compound.

Under cathodic and anodic polarization, the addition of benzene, phenol or aniline increases the corrosion current density. An increase in the cathodic and anodic currents without noticeable change in the corrosion potential with respect to the blank was observed. With such compounds, calculated $E(\%)$ values were found to be negative, showing that the

Table 1. Electrochemical parameters of the amorphous alloy FeBSiC electrode in 1 M HCl; in 1 M HCl + added different organic products (10^{-4} M) and the corresponding corrosion inhibition efficiency

Electrolyte	E_{cor} /mV vs SCE	I_{cor} /$\mu A\ cm^{-2}$	b_c $mV\ dec^{-1}$	E %
1 M HCl	−450	94	165	–
1 M HCl + 10^{-4} M DOAPD	−350	08	150	91.5
1 M HCl + 10^{-4} M OATP	−360	20	150	79
1 M HCl + 10^{-4} M phenol	−440	100	140	−6
1 M HCl + 10^{-4} M aniline	−440	100	140	−6
1 M HCl + 10^{-4} M benzene	−440	120	150	−27

corrosion of the FeBSiC electrode is accelerated. These results indicate that benzene, phenol and aniline have a catalytic effect, both on the hydrogen reduction rate, as well as on the metal dissolution.

In 1 M HCl, the addition of 10^{-4} M of OATP or DOAPD decreases the cathodic current. However, the decrease occurring in the presence of OATP is smaller. The corrosion potential, E_{corr}, of the FeBSiC alloy shifts toward anodic values in the presence of DOAPD and OATP. The corrosion inhibition efficiency with a concentration of 10^{-4} M of the former is 91.5% and of the latter is 79%.

An important observation is that the addition of both DOAPD and OATP at the critical concentration, 10^{-4} M, results in a potential dependent decrease in the cathodic currents (see Fig. 1(a)). The cathodic corrosion inhibition efficiency becomes less significant when the electrode potential shifts towards very negative values.

In the anodic domain, for overvoltages higher than −300 mV vs SCE, the presence of DOAPD or OATP does not appear to change the current-potential characteristics (Fig. 1(b)). This means that the inhibition mode of these compounds depends on the electrode potential. For very positive potential values, the inhibiting character of both DOAPD and OATP disappears. The corrosion inhibition of both DOAPD and OATP is essentially cathodic.

The corrosion inhibition efficiency of the studied organic compounds was found to be in the following order:

DOAPD > OATP > aniline = phenol > benzene

4. Electrochemical impedance measurements

To obtain a better understanding of the interaction mechanism between DOAPD molecules and the amorphous alloy in HCl, impedance measurements at the interface were carried out. Results are presented in Figs 2–4 as Nyquist plots. The different parameters resulting from the analysis of these diagrams are as follows:

(i) resistance of the electrolyte, R_e and of the electrochemical polarization, R_p, respectively, defined by the limit of the real part of the diagram of Nyquist at infinite and zero frequencies,

(ii) charge transfer resistance, R_T, determined from the diameter of the capacitative loop [12, 13],

(iii) the capacity of the double layer deduced from the relation $C^{-1} = 2\pi f_m R_T$, where f_m is the frequency corresponding to the maximum capacity arc at $R_T/2$.

The impedance diagram obtained with 1 M HCl given in Fig. 2 only shows one flat capacitative loop. At low frequencies, the presence of capacitative and inductive loops can be attributed to the adsorption of species resulting from the alloy dissolution and to the adsorption of hydrogen [12, 14]. When 10^{-4} M DOAPD is added to the molar HCl, the Nyquist diagram in Fig. 3 presents only a flat capacitive loop. The impedance values are much higher than values noted for the alloy in the absence of inhibitor. When the DOAPD concentration is increased from 10^{-4} to 10^{-2} M, the Nyquist diagram again displays one capacitive and one inductive loop (Fig. 4). Impedance values with 10^{-2} M DOAPD were found to be significantly smaller than those with the blank.

Such a reduction in corrosion inhibition efficiency above a critical inhibitor concentration was reported for iron in acidic solutions inhibited by acetylenic alcohol [12]. Values of R_p, R_t and C, as well as the corrosion inhibition efficiency of DOAPD, are given in Table 2. The corrosion inhibition efficiency determined from impedance measurements is compared to that deduced from electrochemical steady state and gravimetric methods. The corrosion inhibition efficiency is calculated from the impedance measurements according to the relation

$$E = (I - R_t'/R_t) \times 100 \qquad (2)$$

R_t' and R_t represent, respectively, the charge transfer resistance of the studied alloy before and after the addition of DOAPD to the corrosive medium. R_t is related to the corrosion current density by [12, 13]

$$i = kR_t^{-1} \qquad (3)$$

where k is a constant. From the analysis of data given in Table 2, the following observations can be made:

(i) On addition of 10^{-4} M DOAPD, the capacity diminishes indicating that some molecules are probably adsorbed on the alloy surface.

(ii) Polarization and charge transfer resistances, R_p and R_t, increase in the presence of 10^{-4} M DOAPD. The value of the corrosion inhibition efficiency, 95.1%, calculated on the basis of R_t values, was more or less the same as values determined from electrochemical steady state and gravimetric methods (Table 2).

(iii) From impedance data the corrosion inhibition efficiency in the presence of 10^{-2} M DOAPD was found to be negative contrary to the corrosion inhibition efficiency (12%) found for the same concentration from steady-state electrochemical and gravimetric methods. Epelboin *et al.* [12], studying inhibition by propalgylic alcohol, have noticed a similar result.

In Table 3, the electrochemical parameters deduced from impedance measurements as a function of the immersion time in the aggressive medium containing DOAPD prior to measurements, are given. Clearly increasing the immersion time results in an increase in the charge transfer, R_t, and polarisation, R_p, resistances. The capacity value is independent of immersion time.

5. Discussion

Electrochemical steady state and transient measurements of the behaviour of FeBSiC/HCl and FeBSiC/HCl + DOAPD interfaces indicated that the

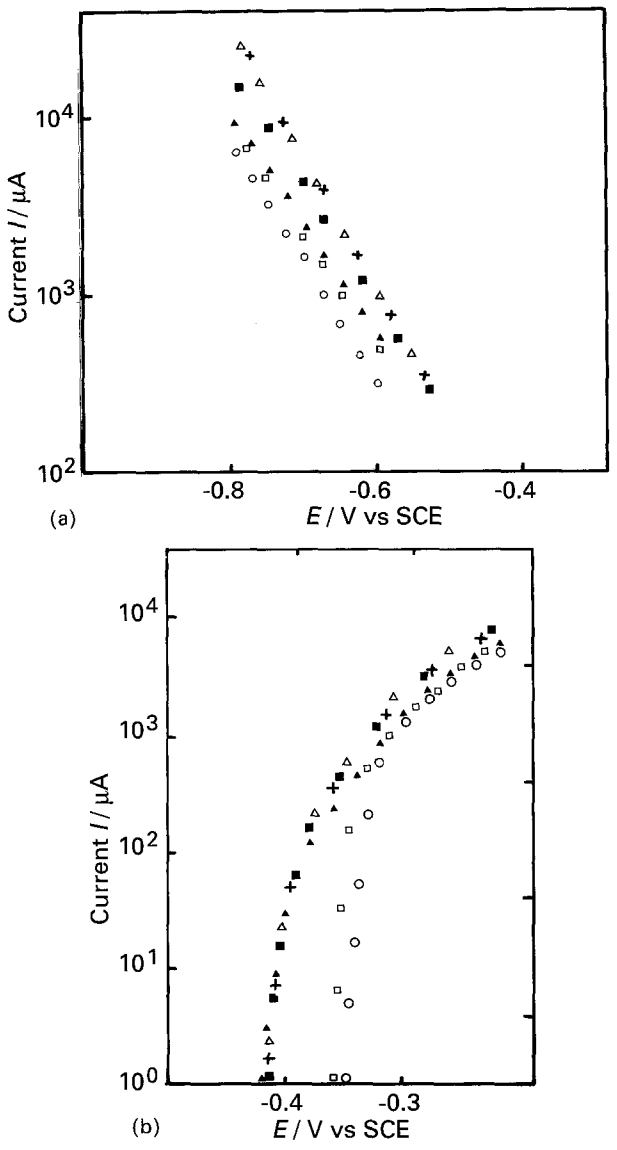

Fig. 1. Current–potential characteristics upon cathodic (a) and anodic (b) polarizations of the amorphous FeBSiC alloy in 1 M HCl and 1 M HCl + 10^{-4} M of different organic compounds: (▲) 1 M HCl; (○) HCl + DOAPD: (□) HCl + OATP; (+) HCl + aniline; (△) HCl + phenol; (■) HCl + benzene. The area of the working electrode is 0.7 cm^2.

DOAPD up to 10^{-4} M inhibits both the corrosion of the alloy and the penetration of hydrogen. For a cathodically charged alloy, numerous blisters due to hydrogen penetration in the alloy are observed. The presence of DOAPD significantly reduces the number of hydrogen blisters on the charged amorphous surface [9, 10]. DOAPD acts on the cathodic process without changing the hydrogen reduction mechanism. The preponderant cathodic effect is explained by a decrease of the active surface area due to the adsorption of DOAPD molecules which replace the hydrogen ions, effectively resulting in a significant fraction of the alloy surface being covered. In fact, in the presence of 10^{-4} M DOAPD, the inductive loop associated with metal dissolution and hydrogen adsorption is not observed on the Nyquist diagram (see Fig. 3 and compare with the inductive loop noted on Fig. 2 for the base electrolyte).

The corrosion inhibition efficiency depends on inhibitor concentration up to 10^{-4} M. It seems that DOAPD does not show a corrosion inhibition effect at electrode potentials higher than −300 mV vs SCE (Fig. 1(b)). This potential can be defined as the desorption potential. The same result has been reported with other organic compounds [15–19]. In cases where the corrosion inhibition depends on inhibitor concentration and on the electrode potential, the observed inhibition phenomenon is generally described as corrosion inhibition of the interface associated with the formation of bidimensional layer adsorbed on the electrode surface [19]. The behaviour of DOAPD at potentials higher than −300 mV vs SCE may be the result of significant alloy dissolution leading to a desorption of the DOAPD inhibitor from the electrode surface. In this case the desorption rate of the DOAPD inhibitor is higher than its adsorption rate. However, DOAPD manifests a corrosion inhibition efficiency over a large anodic domain up to 1000 mV vs SCE with the FeCrPSiC amorphous alloy in the same corrosive medium HCl [20]. This implies that the inhibition effect of DOAPD is related to the elemental composition of the alloy.

The decrease of DOAPD corrosion inhibition observed at concentrations higher than 10^{-4} M was discussed elsewhere [9, 10]. We will now discuss and interpret this effect by a model describing the surface coverage with DOAPD molecules.

The comparative study of corrosion inhibition of 10^{-4} M aromatic compounds indicates that DOAPD and OATP have a much more significant effect. This implies that the essential effect of the corrosion inhibition is due to the presence of electron donor groups (S, N, aromatic cycle) in the molecular structure. This phenomena of intra-molecular complementarity between the different electron donor groups leads to a better corrosion inhibition efficiency. The presence of free electron pairs in the sulphur atoms and of electrons on aromatic nuclei favours the adsorption of the inhibitor.

This configuration has been demonstrated in the case of OATP [21]. The DOAPD is a more efficient corrosion inhibitor than the other organic compounds studied because its two sulphur atoms, two

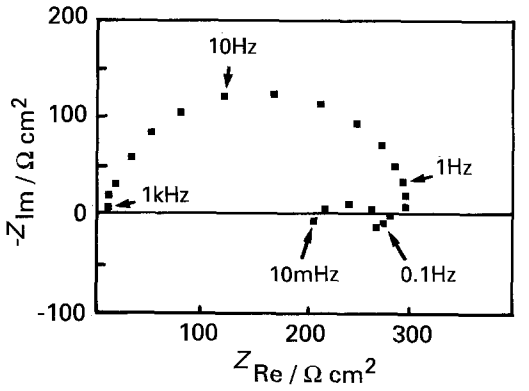

Fig. 2. Electrochemical galvanostatic impedance diagram of the amorphous alloy electrode FeBSiC in molar HCl after 40 min immersion at E_{cor} prior to measurements. The working electrode area was 0.7 cm^{-2}.

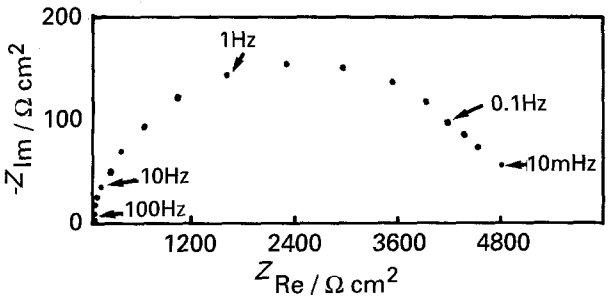

Fig. 3. Electrochemical galvanostatic impedance diagram of the amorphous alloy electrode FeBSiC in molar HCl + 10^{-4} M DOAPD after 40 min immersion at E_{cor} prior to measurements.

nitrogen atoms and two aromatic centres give it an important molecular surface, and several sites with favourable electron densities for preferential adsorption interactions.

In strongly acidic media, the amino acid groups of the DOAPD molecule are likely to be protonated as shown:

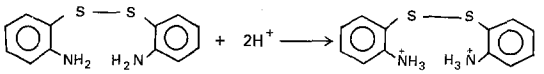

The adsorption of the protonated form of DOAPD is favoured by the attractive interaction between the Cl^- anions and the cations of the inhibitor $(S-C_6H_4-N^+H_3)_2$. This complimentary effect was already observed in acid solutions containing Cl^- Br^-, I^- and inhibitor cations as (ammonium quaternary), pyridinium ions and amines [22–24]. The adsorption of the ionic form $(S-C_6H_4-N^+H_3)_2$ depends on the concentration of the adsorbed chloride anions [10]. Schmitt *et al.* have reported that the adsorption of ammonium quaternary ions on Fe in HCl occurs (cooperatively and competitively) with Cl^- anions [25]. These authors pointed out that the corrosion inhibition efficiency is maximum in the case of cooperative adsorption where the inhibitor cations are adsorbed on the surface which has previously been covered by Cl^- anions. However, Steiner *et al.* have shown by ESCA analysis that dibutylthiourea dissociates and then chemisorbs with the formation of FeS onto the surface of a steel (ST(3))

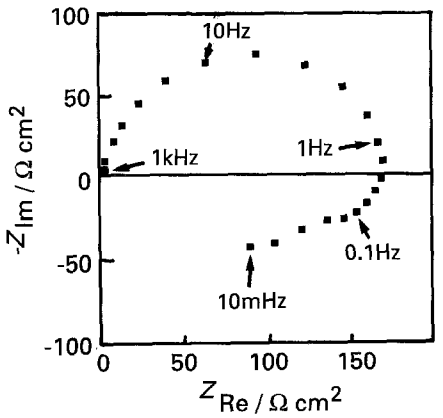

Fig. 4. Electrochemical galvanostatic impedance diagram of the amorphous alloy electrode FeBSiC in molar HCl + 10^{-2} M DOAPD after 40 min immersion at corrosion potential prior to measurements.

electrode in HCl 12% [26]. The hydrocarbon/hydrophobic fragments of the molecules are concentrated near the electrode surface while the chemisorption of fragments containing nitrogen atoms is weak.

When the different models of DOAPD adsorption are considered, the following scenarios are possible:

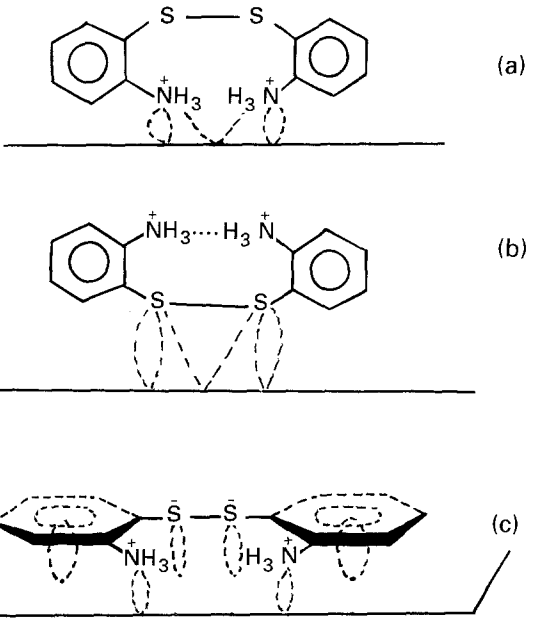

The models are likely to be very unstable, first because of steric hindrance of the molecule and, second, because of intermolecular interactions giving rise to different deformations. Model (c) is stable and preferred since the covered fraction of the surface is high, even at low concentrations, and thus explains the cathodic effect of the DOAPD. This adsorption model is favoured by establishing 'donor–acceptor' links between the empty d orbitals of Fe and the pairs of free electrons on sulphur atoms, as well as the electrons of aromatic rings, also by the electrostatic interactions between the N^+H_3 group and the Cl^- adsorbed anions on the surface.

The increase in the surface coverage with increase in concentration may be illustrated by the following representation:

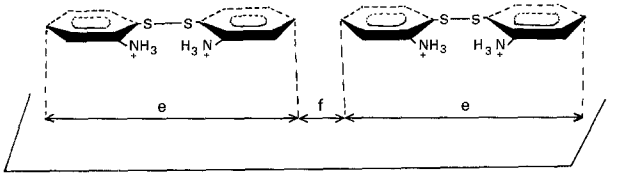

In this case two pictures of the surface may be envisaged:

1. A fraction of the surface is covered with adsorbed DOAPD molecules with cathodic and anodic sites.
2. The non-covered surface is in direct contact with the electrolyte. On this fraction of the electrode surface, the hydrogen reduction reaction occurs justifying the non modification of the mechanism upon the addition of DOAPD.

Table 2. Electrochemical impedance parameters of the amorphous allloy FeBSiC electrode in 1 M HCl; in 1 M HCl + DOAPD. Immersion time was 40 min at $i = 0$

Electrolyte	R_p $\Omega\,cm^{-2}$	R_t $\Omega\,cm^{-2}$	C $\mu F\,cm^{-2}$	E_1^* %	E_2^* %	E_3^* %
1 M HCl	180	300	70	–	–	–
1 M HCl + 10^{-4} M DOAPD	4800	4800	32	94	91.5	88
1 M HCl + 10^{-2} M DOAPD	80	180	130	−66	15	11

* E_1, E_2 E_3 are, respectively, the corresponding corrosion inhibition efficiency determined from impedance measurements, extrapolation of Tafel line and gravimetric technique

The adsorption of DOAPD, which gives rise to an excellent corrosion inhibition and opposes hydrogen penetration into the alloy, must necessarily be followed by a molecular stacking on the surface.

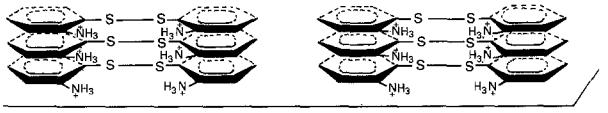

In the first case, the establishment of a stable and relatively thick inhibition layer as illustrated by the last picture, leads to a high corrosion inhibition efficiency at high DOAPD concentration.
In the second case, the increase in DOAPD concentration, modifies the mode of adsorption corresponding to model (a) and/or model (b), as illustrated earlier, thus giving rise to a decrease in the corrosion inhibition efficiency. The increase of inhibitor concentration can lead to a reorientation of adsorbed species responsible for the corrosion inhibition effect. This phenomenon of reoriented organic molecules has been reported elsewhere by many authors [27–30].

6. Conclusions

The steady-state measurements have shown that the hydrogen evolution reaction on the alloy surface occurs according to an activation mechanism only. The added organic compounds do not change the proton reduction mechanism. The presence of 10^{-4} M of aniline, benzene or phenol leads to a catalytic effect on both the alloy dissolution and hydrogen reduction reaction.

With 10^{-4} M of DOAPD or OATP a cathodic inhibition effect occurred. This inhibition effect is potential dependent and its maximum value is attained at the corrosion potential.

Table 3. Influence of immersion time (prior to measurements) of the electrode FeBSiC in 1 M HCl + 10^{-4} M DOAPD on the impedance parameters

Time of immersion	$R_p = R_T/\Omega\,cm^2$	$C/\mu F\,cm^{-2}$
40 min	4800	32
3 h	8400	31
5 h 30 min	9600	33
6 h 40 min	10800	30

The inhibition efficiency of the organic compounds studied can be classified in the following order:

DOAPD > OATP > aniline = phenol > benzene

The electrochemical impedance measurements have shown that the addition of DOAPD to the corrosive medium modify the aspect of the diagrams and the modifications occurring are inhibitor concentration dependent. Upon the addition of 10^{-4} M DOAPD to the base electrolyte (HCl), the increase in the impedance is accompanied by a decrease in the capacity. This effect is more significant when the immersion time is increased. The inhibition efficiency of 10^{-4} M DOAPD calculated from transient measurements is consistent with values calculated from both steady-state and weight loss methods. The increase of DOAPD concentration up to 10^{-2} M gives rise to a decrease in the impedance and of the inhibition efficiency and to an increase in the capacity.

The cathodic corrosion inhibition of DOAPD is interpreted by a blocked fraction of the electrode surface due to the adsorption of protonated species on the surface. Hydrogen reduction occurs on the electrode surface which is not blocked by the inhibitor.

A model for the covered alloy surface by DOAPD inhibitor is proposed. This model demonstrates the effect of DOAPD as a corrosion and hydrogen surface embrittlement inhibitor for the alloy.

Acknowledgements

The authors are indebted to Drs Robert Reeves and Michel Keddam for fruitful and stimulating discussions. Impedance measurements were carried out in the Laboratoire de Physique de Liquides et Electrochimie, Université Paris VI, 4, Place Jussieu 75252 Paris Cédex. The help of Dr H. Takenouti during these measurements is gratefully acknowledged.

References

[1] A. Kawashima, K. Hashimoto and T. Masumoto, *Corros. Sci.* **16** (1976) 935.
[2] K. Hashimoto, K. Osada, T. Masumoto and S. Schimodaria, *ibid.* **16** (1976) 71.

[3] J. Crousier, J. P. Crousier, Y. Massiani and C. Antonione, *Gazzetta Chimica Italiana* **113** (1983) 329.
[4] M. Da Cunha Belo, B. Rondot and E. Navaro, *Métaux Corrosion Industrie* **658** (1980) 02.
[5] N. Nagumo and T. Takahashi, *Mater. Sci. Eng.* **23** (1976) 257.
[6] R. K. Viswanadham, J. A. S. Green and W. G. Montague, *Scr. Metall.* **10** (1976) 229.
[7] M. Naka, K. Hashimoto and T. Masumoto, *Corrosion* **32** (1976) 146.
[8] R. B. Diegle, *ibid.* **35** (1979) 35.
[9] S. Kertit, J. Aride, A. Ben-Bachir, A. Srhiri, A. Elkholy and M. Etman, *J. Appl. Electrochem.* **19** (1989) 83.
[10] *Idem, ibid.* **19** (1989) 512.
[11] J. Aride, A. Ben-Bachir, K. Elkacemi, M. Etman, S. Kertit and A. Srhiri, *J. Chim. Phys.* **88** (1991) 631.
[12] I. Epelboin, M. Keddam and H. Takenouti, *J. Appl. Electrochem.* **2** (1972) 71.
[13] I. Epelboin, C. Gabrielli, M. Keddam and H. Takenouti, 'Electrochemical Corrosion Testing', ASTM STP 727 (edited by F. Mansfeld and U. Bertocci), American Society for Testing Materials (1991) pp. 150–166.
[14] I. Epelboin, Ph. Morel and H. Takenouti, Cong. Intern. 'L'hydrogène dans les mètaux'. Paris (1972) p. 234.
[15] T. Sayegh, A. Srhiri, A. Ben-Bachir, A. Sayegh and M. Chraibi, 7th Symposium on Corrosion Inhibitors, Ferrara, Italy (1990).
[16] K. Ben-Chekroun, A. Ben-Bachir and A. Elkholy, 6th Symposium on Corrosion Inhibitors, Ferrara, Italy (1985).
[17] J. O'M. Bockris and B. Yang, *J. Electrochem. Soc.* **138 (1991) 2237.**
[18] W. J. Lorenz and F. Mansfeld, *Corros. Sci.* **21** (1981) 647.
[19] W. J. Lorenz and F. Mansfeld, *Electrochim. Acta* **31** (1986) 467.
[20] M. Etman, A. Elkholy, J. Aride, T. Biaz and S. Kertit, *J. Chim. Phys.* **86** (1989) 347.
[21] A. Srhiri, Thèse d'Etat, Université Paul Sabatier, Toulouse (1985).
[22] I. L. Rosenfeld, *in* 'Corrosion Inhibitors', McGraw-Hill, New York, (1981).
[23] R. Driver and R. J. Meakins, *Brit. Corros. J.* **9** (1974) 233.
[24] R. M. Houdson and C. J. Warning, *Corros. Sci.* **10** (1970) 121.
[25] G. Schmitt and K. Bedbur, *Werkst. Corros.* **36** (1985) 273.
[26] P. Steiner, M. Huppert, H. Wern and S. Hufner, *ibid.* **35** (1984) 7.
[27] N. Hackereman, D. D. Justice and E. McCafferty, *Corrosion* **31** (1975) 240.
[28] T. Smith, *J. Colloid & Interface Sci.* **28** (1968) 531.
[29] J. F. Scamehorn, R. S. Schechter and W. A. Wade, *ibid.* **85** (1982) 463.
[30] O. Ikeda, F. Goto and H. Tamura, *Bull. Chem. Sci. Japan* **54** (1981) 3146.